CCFE-PR(15)74

Zbigniew Mitura and Sergei L. Dudarev

Algorithms for determining the phase of RHEED oscillations

Algorithms for determining the phase of RHEED oscillations

Zbigniew Mitura[a] and Sergei L. Dudarev[b]

[a]AGH University of Science and Technology, Faculty of Metals Engineering and Industrial Computer Science, al. Mickiewicza 30, 30-059 Kraków, Poland

[b]CCFE, Culham Science Centre, Oxfordshire OX14 3DB, UK

Algorithms for determining the phase of RHEED oscillations

Zbigniew Mitura[a]* and Sergei L. Dudarev[b]

[a]*AGH University of Science and Technology, Faculty of Metals Engineering and Industrial Computer Science, al. Mickiewicza 30, 30-059 Kraków, Poland, E-mail: mitura@metal.agh.edu.pl, and* [b]*CCFE, Culham Science Centre, Oxfordshire OX14 3DB, UK*

Abstract

Oscillations of reflection high energy electron diffraction (RHEED) intensities are computed using dynamical diffraction theory. The phase of oscillations is then determined using two alternative approaches. In the first approach, the phase is found by directly examining the intensity oscillation data. In the second approach, the phase is determined using harmonic analysis. We compare the two methods and apply them to the determination of the phase of RHEED oscillations observed experimentally. For the incident beam azimuths corresponding to low symmetry directions both approaches produce similar results, showing that either algorithm can be used in applications.

1. Introduction

Reflection high energy electron diffraction (RHEED) is a robust and convenient technique for monitoring growth of nanostructures. Recent examples of structures produced using RHEED as a monitoring tool include: Au nanoparticles (Chen *et al.*,

2013), GaAs:Mn nanowires (Sadowski *et al.*, 2007), biaxial W nanorods (Krishnan *et al.*, 2010) and Ge layers on a GaAs substrate (Ohtake *et al.*, 2009). In most cases the interpretation of experimental RHEED data involves highly simplified assumptions. This is largely because quantitatively accurate models for predicting RHEED intensities, based on dynamical diffraction theory, were developed only for flat surfaces, see Ichimiya & Cohen (2004), and Peng *et al.* (2004), with theoretical effort also addressing the problem of electron absorption and diffuse scattering by random arrangements of atoms on a growing surface or randomly distributed surface steps (Dudarev *et al.*, 1992; Dudarev *et al.*, 1994; Dudarev, 1997). RHEED became broadly accepted as a useful tool for monitoring surface structure of growing crystals after the discovery of oscillating changes of intensity of electron beams reflected from the surface during crystal growth, first reported by Wood (Wood, 1981) and Harris *et al.* (Harris *et al.*, 1981), see Herman & Sitter (1996) for more detail. The period of such intensity variations, called RHEED oscillations, corresponds to the deposition of one new monolayer onto a surface during growth. In the 1980's, RHEED oscillations were observed during molecular beam epitaxial growth where experiments were performed in ultra-high vacuum. More recently, RHEED intensity oscillations were observed at gas pressures considerably higher than the pressure characterizing molecular beam epitaxy conditions. For example, oscillations were recorded during pulsed laser deposition (Rijnders *et al.*, 1997; Li *et al.*, 2012). Several theoretical models for RHEED oscillations have been developed (Pukite *et al.*, 1988; Holmes *et al.*, 1997; Peng & Whelan, 1990) since the discovery of the effect, however the range of validity of these models is limited. The subject has again attracted attention recently (Vasudevan *et al.*, 2014; Sullivan *et al.*, 2015).

In this paper we focus on algorithms for processing RHEED oscillation data, and specifically on the determination of generic parameters characterizing the oscillations.

For example, if we assume the availability of data describing some statistically representative oscillation data sets, we can characterize them by introducing parameters like the amplitude of oscillations, their phase, the decay time constant etc. The values of such parameters can be determined through a direct examination of oscillating intensity curves and matching the data to a chosen functional form.

An alternative approach would be to use the Fourier analysis, as this would enable filtering out fluctuations of intensity oscillations. In general, the interpretation of intensity oscillations and analysis of data can be quite complex. In this paper we focus on a particular problem of comparing the phase of experimentally observed oscillations with the phase of oscillations predicted theoretically assuming perfect layer-by-layer growth. RHEED oscillations observed experimentally are usually relatively smooth, as shown in Fig. 1, and their phase can be readily determined by identifying the time point corresponding of the intensity minimum in the second period of oscillations. However, the curves computed using models based on dynamical diffraction theory may potentially have fairly complex shape, as illustrated in Fig.2, and this is why it would be illuminating to compare the outcomes of analysis performed using a direct approach and the Fourier decomposition method.

This work extends studies described in Mitura *et al.* (1998) and Mitura *et al.* (2002). In our earlier work the phase of oscillations derived directly from experimental data was compared with the phase computed using dynamical diffraction theory and then analyzed using using the Fourier transform method. Here, we extract phase information from curves, computed using dynamical diffraction theory, using two complementary approaches: first directly from the curves and then by harmonic analysis. Before proceeding to the interpretation of experimental data we assess the advantages and disadvantages of both methods. We also use a different model for describing crystal growth. Previously, we assumed that the surface was reconstructed, now we ignore

surface reconstruction but take into account that the amplitudes of thermal displacements of Ga and As atoms may differ. Also, here we use a somewhat different definition of the oscillation phase. In the earlier papers we assumed that the values of the phase were in the range $[-\pi;\pi]$, presently the values are in the range from 1 to 2, as in (Zhang *et al.*, 1987) and (Joyce *et al.*, 1988).

The paper is organized as follows. In Sec. 2 we describe the two approaches to the determination of the phase and apply them to the analysis of intensity oscillations predicted using dynamical diffraction theory. In Sec. 3 we analyze experimental observations and in Sec. 4 we present our conclusions.

2. Two approaches to the determination of RHEED oscillation phase

We assume that for each glancing angle of incidence we can find the intensity of specular reflection from a dynamical diffraction calculation, as it is shown for example in Mitura *et al.* (1998) and Mitura *et al.* (2002). We are interested in analyzing RHEED intensities for the azimuthal orientations of the incident beam that are off the high symmetry directions. For such orientations the intensity of the specular beam is almost insensitive to the lateral periodicity of the surface. Hence the effective potential describing interaction of high energy electrons with atoms can be assumed to depend only on the coordinate in the direction normal to the surface, see (Dudarev *et al.*, 1992). This diffraction geometry is often referred to as the one-beam RHEED condition.

We assume that the potential in the growing layer of atoms is given by the potential of a complete atomic layer multiplied by surface coverage Θ, where $0 < \Theta < 1$. For each glancing angle, surface coverage varies on a mesh of values defined by the number of points N_{cov} for which, over one oscillation period, RHEED intensities are computed. Over an oscillation period, the values of coverage Θ for which RHEED intensities

are computed are $0, 1/N_{cov}, 2/N_{cov}, ..., (N_{cov}-1)/N_{cov}$. Assuming perfect layer-by-layer growth, for each glancing angle we vary Θ and compute the individual RHEED intensity-versus-time (i.e. intensity versus surface coverage) oscillation curves.

We investigate growth of atomically thin GaAs layers on the (001) GaAs surface. No reconstruction of the surface is assumed. The energy of electrons is 10 keV. Results shown in Sec.2 refer to dynamical diffraction calculations where the potential of interaction between electrons and the atoms is evaluated ignoring thermal atomic vibrations.

2.1. Direct determination of the phase

According to Zhang *et al.* (1987) and Joyce *et al.* (1988) the phase of oscillations can be defined "as the time taken to reach the second oscillation minimum normalized by the time of a complete period". The authors of the above papers introduced a symbol $t_{3/2}/T$ to denote this quantity. For cases shown in Fig.1 and Fig.2a their definition can be readily applied, and one expects that the phase defined in this way would span the range from 1 and 2. However, if multiple intensity minima are observed over a period, as shown in Fig.2b, then the definition proposed in Zhang *et al.* (1987) causes confusion. To make sure that condition $1 \leq t_{3/2}/T < 2$ is satisfied even for cases where oscillations exhibit multiple minima over each oscillation period, we modify the definition given in Zhang *et al.* (1987). We define $t_{3/2}$ as the time point corresponding to the lowest value of intensity over the second period of oscillations, and then define the oscillation phase by dividing the resulting value by T. The phase computed in this way is denoted by $(t_{3/2}/T)_{dir}$.

The use of the above definition for $(t_{3/2}/T)_{dir}$ when interpreting experimentally observed oscillations does not cause any difficulty as oscillating intensity can be recorded as a continuous function of time. The curves computed theoretically are

somewhat more difficult to interpret as they are computed on a discrete set of points where each point corresponds to a certain value of N_{cov}.

The phase computed using the formula $(t_{3/2}/T)_{dir}$ are shown in Fig.3. The plots were produced using several different values of N_{cov}. The fact that the intensities are computed for a discrete set of surface coverages $\Theta = (0, 1/N_{cov}, ..., (N_{cov} - 1)/N_{cov})$ results in that the curves do not look like smooth functions. Although in principle we are interested in the limit $N_{cov} \rightarrow \infty$, the curve computed for $N_{cov} = 20$ already provides a reasonably accurate approximation.

2.2. Determination of the phase using harmonic analysis

Whereas an algorithm for determining the phase directly from RHEED intensity curves may be applied successfully to simple cases, it would be desirable to introduce a more general definition for the phase, especially given that any experimentally observed curve involves small intensity fluctuations that need to be filtered out. This can be achieved using the Fourier analysis. Any periodic function $f(t)$, where $f(t) = f(t+T)$ and T is the period, can be represented by a series as follows (Mitura *et al.*, 1998; Mitura *et al.*, 2002)

$$\begin{aligned} f\ (t) \quad &= \quad \frac{1}{2}A_0 \ + \ A_1 \ \cos\left(\frac{2\pi}{T}\ t - \phi_1\right) \ + \\ &+ \quad \left[\sum_{n=2}^{\infty} \ A_n \ \cos\left(n\ \frac{2\pi}{T}\ t - \phi_n\right)\right] \ , \end{aligned} \tag{1}$$

where we assume that $A_n \ \geq \ 0 \quad \text{for} \quad n \geq 1$. The terms corresponding to $n \geq 2$ can be filtered out and ignored. Since A_0 is a constant, we see that the shape of oscillations can be described by only two parameters, A_1 and ϕ_1. Appendix A shows how these two parameters can be found in practice.

We now compare values derived from a direct examination of oscillations with those deduced using harmonic analysis. For oscillations with simple, cosine-like, function shape the values computed using the two approaches should be expected to be very

close. To ensure this, we need to introduce a normalization convention. For example, we may compare values of ϕ_{dir} defined as $\phi_{dir} \equiv 2\pi[(t_{3/2}/T)_{dir} - 1.5]$ and ϕ_{harm} defined as $\phi_{harm} \equiv \phi_1$ (Mitura *et al.*, 1998; Mitura *et al.*, 2002). In the current paper we adopt a convention that matches the range of variation of the phase given in Zhang *et al.* (1987) and Joyce1988.

In what follows we assume that the phase $(t_{3/2}/T)_{dir}$ defined in Sec.2.1 is equivalent to $(t_{3/2}/T)_{harm}$ defined as follows

$$(t_{3/2}/T)_{harm} \equiv \phi_1/(2\pi) + 1.5, \tag{2}$$

where ϕ_1 is the phase entering Eq.(1).

It is illuminating to see how the values of the phase defined using the Fourier analysis depend on the number of mesh points N_{cov} used in RHEED intensity calculations. Three plots of phase $(t_{3/2}/T)_{harm}$ computed using various values of N_{cov} are shown in Fig.4. All of them are smooth and it appears that the plot computed for $N_{cov} = 8$ already approximates well the limit $N_{cov} \to \infty$.

2.3. Analysis of oscillations

In this section we compare phases of oscillations derived using the two methods outlined above. As a test, we apply the phase determination algorithms to the intensity oscillation curves computed theoretically using dynamical diffraction theory. To produce the curves shown in Fig. 5, we first compute RHEED intensity oscillation curves assuming an off-symmetry azimuth and using dynamical diffraction theory as explained at the beginning of Sec.2. Then, the phases of oscillations were determined as described in Sec.2.1 and Sec.2.2. In both cases, the number of mesh points N_{cov} used in calculations when approximating surface coverage during growth was equal to 20.

Fig.5 shows that the two plots are fairly similar, and differ only over relatively

narrow intervals of angles of incidence: from 1.9° to 2.5°, from 4.6° to 5.0°, and from 7.2° to 7.4°. We note that despite the fact that in the above intervals the values of phases appear different, in fact the difference is not materially significant since the phase only enters an expression for an observable quantity (intensity of the specular beam) through an argument of a periodic function.

To clarify the point we consider two sets of cosine-like oscillations that have the same period T, but are characterized by slightly different positions of the intensity minima. If we assume that the first set of oscillations has minima at $t = 1.02T$ whereas the minima of the second set are at $t = 0.99T$, we can say that in general both sets are nearly identical. If we apply the direct method of phase determination to the two sets we discover that for the first set the value of the phase is 1.02 whereas the value of the phase derived from the second set is 1.99. The reason for the somewhat unexpectedly large value of the phase in the latter case is that the intensity minimum occurring during the first period of oscillations $t = 0.99T$ is not taken into account in the analysis. Physically there is no difference between the values of 0.99 or 1.99, and the example illustrates that the direct analysis may deliver discontinuous values if the phase is close to one of the boundaries of the interval $[1, 2]$.

Still, from the examination of Fig.5 we conclude that the plot of the phase derived using the Fourier analysis is similar to the plot derived from a direct examination of oscillations.

3. Interpretation of experimental data

In this section we focus on the interpretation of experimental data. The experimental phase points shown in Figs. 6-7 are taken from literature (Crook *et al.*, 1989) where the values were derived by directly examining the oscillation data. Theoretical plots shown in Figs.6-7 illustrate the angular dependence of the two phases, defined respectively

in Sec.2.1 and in Sec.2.2.

Theoretical results shown in Figs.6-7 were derived assuming that the surface of the growing layer was not reconstructed (i.e. the surface structure corresponded to a bulk terminated crystal with As atoms forming the top layer). We assumed that there was a small delay associated with the start of MBE growth noted in Osaka *et al.* (1995). Therefore, a constant values of 0.25 was added to all the initial values of theoretically determined phases, i.e. the phases found computationally using the perfect layer-by-layer model of MBE growth. All the results shown in Fig.6. correspond to scattering potential evaluated ignoring thermal vibrations of atoms. Thermal vibrations were taken into account in calculations illustrated in Fig.7. The Debye-Waller factor B for Ga was set to be equal to 2.0 Å^2, and for As it was taken as 2.7 Å^2 . The objective of using different values of B is to take into account the fact that the amplitude of thermal vibrations of atoms at the surface is greater than in the crystal bulk. To retain the simplicity of the model we assumed that there is only one value of B characterizing all the Ga atoms and, similarly, only one value of B characterizing all the As atoms.

The Debye-Waller factors for Ga and As atoms in a perfect crystal at the temperature similar to the temperature of MBE growth are $B_{Ga} = 1.85\mathring{A}^2$ and $B_{As} = 2.00\mathring{A}^2$ (Reid, 1983). The fact that the Debye-Waller factors of Ga and As atoms are different is significant, since this has a strong effect on the effective potential of interaction between high energy electrons and the layers of Ga and As atoms parallel to the surface. The atomic numbers of Ga and As are similar (Z=31 and 33, respectively) and hence the difference between Debye-Waller factors has a particularly strong effect on the temperature-dependent reflectivity of crystal surfaces.

Figs. 6 and 7 shows that both theoretical plots agree with experimental observations rather well. Therefore, both methods for the determination of phases of RHEED oscillations appear suitable for the interpretation of experimental data for the directions

of incidence where one-beam conditions are satisfied.

How do the above conclusions relate to the earlier work (Mitura *et al.*, 1998; Mitura *et al.*, 2002)? When investigating RHEED oscillations in (Mitura *et al.*, 1998; Mitura *et al.*, 2002), we assumed that the growing surface was reconstructed. Also, an extra imaginary part of the scattering potential was included into considerations to account for the losses of electrons resulting from scattering by step edges in the growing layer or by atomic disorder on a growing surface (Dudarev *et al.*, 1992; Dudarev *et al.*, 1994; Dudarev, 1997). The surface reconstruction model known as the $\beta 2(2\times 4)$ model, introduced by Chadi (1987), was used in the calculations performed in (Mitura *et al.*, 1998; Mitura *et al.*, 2002). Taking into account the $\beta 2(2\times 4)$ surface reconstruction seems to be indeed appropriate for the As-rich equilibrium GaAs surfaces, and the use of this reconstruction model in earlier calculations represented a reasonable assumption (Mitura *et al.*, 1998; Mitura *et al.*, 2002).

The real structure of a non-equilibrium surface is more complex, whereas the surface structure formed during growth is still not known in sufficient detail. For example, even at equilibrium, reconstructions different from $\beta 2(2\times 4)$ may form, depending on surface conditions (Ichimiya *et al.*, 2001; Ohtake *et al.*, 2002; Lin & Fichthorn, 2012). Furthermore, Osaka *et al.* (1995) showed experimentally that homoepitaxial growth of GaAs may involve a time delay and suggested that initial ordering of atoms may occur first. Itoh *et al.* (1998) investigated, using Monte Carlo simulations, the formation of surface unit cells, and concluded that intermediate configurations form before the final structure emerges. More recently, some aspects of growth of GaAs were modeled using molecular dynamics (Murdick *et al.*, 2007), who showed that the mode of growth of new atomic layers may indeed be fairly complex.

In this study we decided not to include surface reconstruction effects into consideration, partially for the reason of simplifying the model to assist the most direct

and transparent determination of the phase of oscillations. We have also omitted the imaginary part of the potential associated with atomic disorder in the growing layer (Dudarev *et al.*, 1992), and instead used a model where the imaginary part of the potential was proportional to its real part, see e.g. (Dudarev *et al.*, 1995). Surprisingly, the level of agreement between experimental and theoretical curves shown in Figs. 6-7 is somewhat better than what we found earlier. We would not like to overstate the significance of this improvement. In the first place, the treatment given above confirms that changes in refraction conditions at the surface do have a significant effect on RHEED oscillations. We still observe differences between theoretical predictions and experimental observations, highlighting the desirability of using a more accurate model of growth and a more accurate model for electron scattering for the interpretation of experimental observations.

4. Conclusions

In this paper we compare phases of RHEED intensity oscillations derived from experimental observations, using two alternative approaches to the determination of the phase of oscillations. We found that the phases determined using the two methods were in agreement, although the results were not identical.

Determining the phase directly is a good approach if only a limited amount of experimental information is available. However, the direct method becomes less efficient if a significant amount of data is available. Harmonic Fourier analysis may offer certain advantages in the latter case, particularly given that such analysis makes it possible to filter out fluctuations. In this paper we showed how to apply the Fourier analysis to perfectly periodic oscillations, and there is room for extension of the method, for example to the case of damped oscillations.

Z.M. gratefully acknowledges financial support of this work from the AGH Project

No. 11.11.110.291. The work was also part-funded by the EUROFusion Consortium, and has received funding from Euratom research and training programme 20142018 under Grant Agreement No. 633053, and funding from the RCUK Energy Programme (Grant No. EP/I501045). The views and opinions expressed herein do not necessarily reflect those of the European Commission.

Appendix A
Determination of oscillation phase using harmonic analysis

Below we explain how to find values of A_1 and ϕ_1 in Eq. (1). It is well known that a periodic function $f(t)$ can be represented by a Fourier series

$$\begin{aligned} f\ (t) &= \frac{1}{2}C_0\ + \sum_{n=1}^{\infty}\ \Big[C_n\ \cos{(n\ \frac{2\pi}{T}\ t)} + \\ &+\ S_n\ \sin{(n\ \frac{2\pi}{T}\ t)}\Big], \end{aligned} \tag{3}$$

where

$$C_0 = \frac{2}{T}\int_0^T f(t)dt \tag{4}$$

and, for $n \geq 1$,

$$C_n = \frac{2}{T}\int_0^T f(t)\cos{(n\frac{2\pi}{T}t)}dt, \tag{5}$$

$$S_n = \frac{2}{T}\int_0^T f(t)\sin{(n\frac{2\pi}{T}t)}dt. \tag{6}$$

Using a basic trigonometric relation $\cos(\alpha-\beta) = \cos\alpha\cos\beta+\sin\alpha\sin\beta$, where α and β are real, we transform Eq.(1) as follows

$$\begin{aligned} f\ (t) &= \frac{1}{2}A_0\ + \Big[\sum_{n=1}^{\infty}\ \Big[A_n\ \cos\phi_n\cos{(n\ \frac{2\pi}{T}\ t)} + \\ &+\ A_n\ \sin\phi_n\sin{(n\ \frac{2\pi}{T}\ t)}\Big]. \end{aligned} \tag{7}$$

Comparing terms in Eq.(3) and Eq.(7) we find,

$$A_0 = C_0 \tag{8}$$

and, for $n \geq 1$,

$$A_n \cos\phi_n = C_n, \tag{9}$$

$$A_n \sin\phi_n = S_n. \tag{10}$$

Using Eqs.(9-10) we derive formulae that enable one to compute A_1 and ϕ_1. In Eq.(1) it was assumed that $A_1 \geq 0$. Accordingly, A_1 satisfies the following condition:

$$A_1 = \sqrt{C_1^2 + S_1^2}. \tag{11}$$

Furthermore, since $A_1 > 0$, the magnitude of ϕ_1 can now be found using the following relation:

$$\phi_1 = \begin{cases} \arccos(C_1/A_1) & \text{if } S_1 > 0, \\ -\arccos(C_1/A_1) & \text{if } S_1 \leq 0. \end{cases} \tag{12}$$

It should be mentioned that in the limiting case $A_1 = 0$ the magnitude of ϕ_1 is not defined, but encountering such a limit in practical calculations is not likely.

Eqs. (11-12) can be used to find A_1 and ϕ_1 if the values of C_1 and S_1 are known. Two latter values can be determined using the following formulae:

$$C_1 \simeq \frac{2}{N_{cov}} \sum_{l=0}^{N_{cov}-1} f\Big(\frac{lT}{N_{cov}}\Big) \cos\Big(\frac{2\pi l}{N_{cov}}\Big), \tag{13}$$

$$S_1 \simeq \frac{2}{N_{cov}} \sum_{l=0}^{N_{cov}-1} f\Big(\frac{lT}{N_{cov}}\Big) \sin\Big(\frac{2\pi l}{N_{cov}}\Big). \tag{14}$$

Eqs.(13-14) are the approximate versions of Eqs.(5-6). Namely, Eqs.(13-14) were derived assuming that values of $f(t)$ were defined on N_{cov} discrete points corresponding to a set of discrete time points t.

References

Chadi, D. J. (1987). *J. Vac. Sci. Technol. A*, **5**, 834–837.

Chen, X., Gao, W. P., Sivaramakrishnan, S., Hu, H. F. & Zuo, J. M. (2013). *Appl. Surf. Sci.* **270**, 661–666.

Crook, G. E., Eyink, K. G., Campbell, A. C., Hinson, D. R. & Streetman, B. G. (1989). *J. Vac. Sci. Technol. A*, **7**, 2549–2553.

Dudarev, S. L. (1997). *Micron*, **28**, 139–158.

Dudarev, S. L., Peng, L. M. & Whelan, M. J. (1992). *Surf. Sci.* **279**, 380–394.

Dudarev, S. L., Peng, L. M. & Whelan, M. J. (1995). *Surf. Sci.* **330**, 86–100.

Dudarev, S. L., Vvedensky, D. D. & Whelan, M. J. (1994). *Phys. Rev. B*, **50**, 14525–14538.

Harris, J. J., Joyce, B. A. & Dobson, P. J. (1981). *Surf. Sci.* **103**, L90–L96.

Herman, M. A. & Sitter, H. (1996). *Molecular Beam Epitaxy: Fundamentals and Current Status*. Springer Berlin Heidelberg, 2nd ed.

Holmes, D. M., Sudijono, J. L., McConville, C. F., Jones, T. S. & Joyce, B. A. (1997). *Surf. Sci.* **370**, L173–L178.

Ichimiya, A. & Cohen, P. I. (2004). *Reflection High Energy Electron Diffraction*. Cambridge University Press.

Ichimiya, A., Nishikawa, Y. & Uchiyama, M. (2001). *Surf. Sci.* **493**, 232 – 237.

Itoh, M., Bell, G. R., Avery, A. R., Jones, T. S., Joyce, B. A. & Vvedensky, D. D. (1998). *Phys. Rev. Lett.* **81**, 633–636.

Joyce, B. A., Zhang, J., Neave, J. H. & Dobson, P. J. (1988). *Appl. Phys. A*, **45**, 255–260.

Krishnan, R., Liu, Y., Gaire, C., Chen, L., Wang, G.-C. & Lu, T.-M. (2010). *Nanotechnology*, **21**, 325704.

Li, J., Peng, W., Chen, K., Zhang, Y., Cui, L., Chen, Y., Jin, Y., Zhang, Y. & Zheng, D. (2012). *Solid State Commun.* **152**, 478–482.

Lin, Y. & Fichthorn, K. A. (2012). *Phys. Rev. B*, **86**, 165303.

Mitura, Z., Dudarev, S. L., Peng, L.-M., Gladyszewski, G. & Whelan, M. J. (2002). *J. Cryst. Growth*, **235**, 79 – 88.

Mitura, Z., Dudarev, S. L. & Whelan, M. J. (1998). *Phys. Rev. B*, **57**, 6309–6312.

Murdick, D. A., Wadley, H. N. G. & Zhou, X. W. (2007). *Phys. Rev. B*, **75**, 125318.

Ohtake, A., Ozeki, H., Yasuda, T. & Hanada, T. (2002). *Phys. Rev. B*, **65**, 165315.

Ohtake, A., Yasuda, T. & Miyata, N. (2009). *Surf. Sci.* **603**, 826–830.

Osaka, J., Inoue, N. & Homma, Y. (1995). *Appl. Phys. Lett.* **66**, 2110–2112.

Peng, L.-M., Dudarev, S. L. & Whelan, M. J. (2004). *High-Energy Electron Diffraction and Microscopy*. Oxford University Press.

Peng, L.-M. & Whelan, M. J. (1990). *Surf. Sci.* **238**, L446–L452.

Pukite, P. R., Cohen, P. I. & Batra, S. (1988). In *Reflection High Energy Electron Diffraction and Reflection Electron Imaging of Surfaces*, edited by P. K. Larsen & P. J. Dobson, pp. 427–447. Plenum Press.

Reid, J. S. (1983). *Acta Cryst.* A**39**, 1–13.

Rijnders, G. J. H. M., Koster, G., Blank, D. H. A. & Rogalla, H. (1997). *Appl. Phys. Lett.* **70**, 1888–1890.

Sadowski, J., Dłużewski, P., Kret, S., Janik, E., Łusakowska, E., Kanski, J., Presz, A., Terki, F., Charar, S. & Tang, D. (2007). *Nano Letters*, **7**, 2724–2728.

Sullivan, M. C., Ward, M. J., Gutiérrez-Llorente, A., Adler, E. R., Joress, H., Woll, A. & Brock, J. D. (2015). *Appl. Phys. Lett.* **106**, 031604.

Vasudevan, R. K., Tselev, A., Baddorf, A. P. & Kalinin, S. V. (2014). *ACS Nano*, **8**, 10899–10908.

Wood, C. E. C. (1981). *Surf. Sci.* **108**, L441–L443.

Zhang, J., Neave, J. H., Dobson, P. J. & Joyce, B. A. (1987). *Appl. Phys. A*, **42**, 317–326.

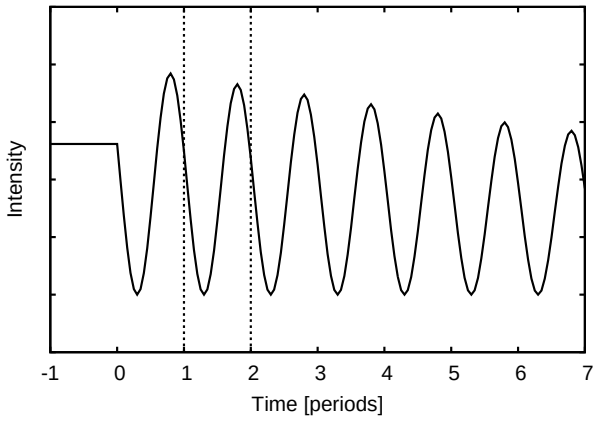

Fig. 1. A typical run of oscillations appearing in experiment. Vertical lines are drawn for $t = T$ and $t = 2T$ to make it easier to recognize intensity changes in the second period of oscillations.

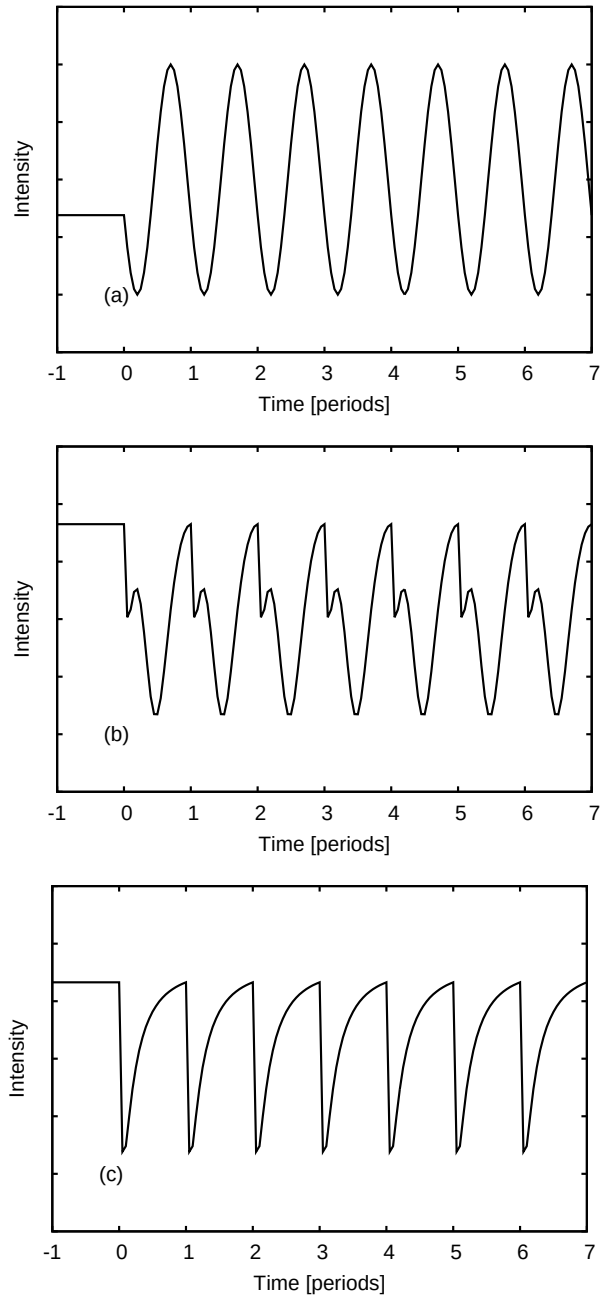

Fig. 2. Runs of oscillations which need to be admitted in theoretical work: (a) oscillations which can be described with the help a cosinus-like function, (b) oscillations with double minima and maxima in one period, (c) the intensity changes which are strongly asymmetric within one period.

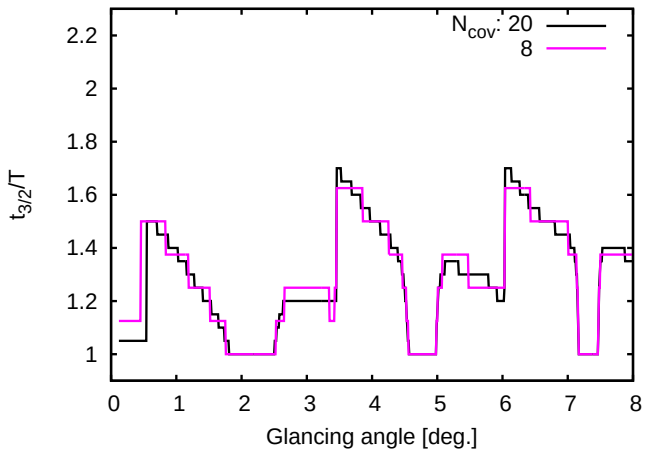

Fig. 3. Plots of the phase found directly from runs of theoretical oscillations for two numbers N_{cov} of coverages considered for the growing layer.

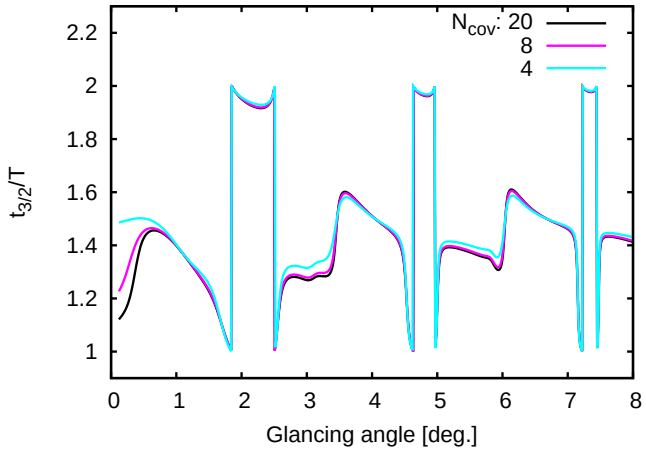

Fig. 4. Plots of the phase determined with the help of the harmonic analysis of theoretical oscillations. The plots are shown for different numbers N_{cov} of coverages assumed for the growing layer.

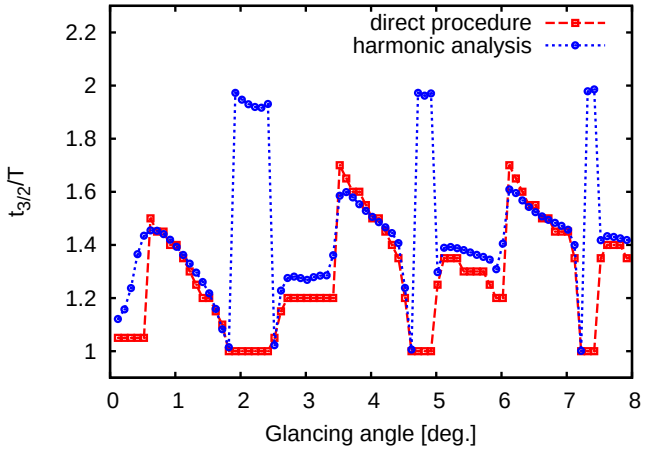

Fig. 5. Plots of the oscillation phase determined using two different methods (direct and employing the Fourier series, respectively) for the identical sets of theoretical oscillations, $N_{cov} = 20$.

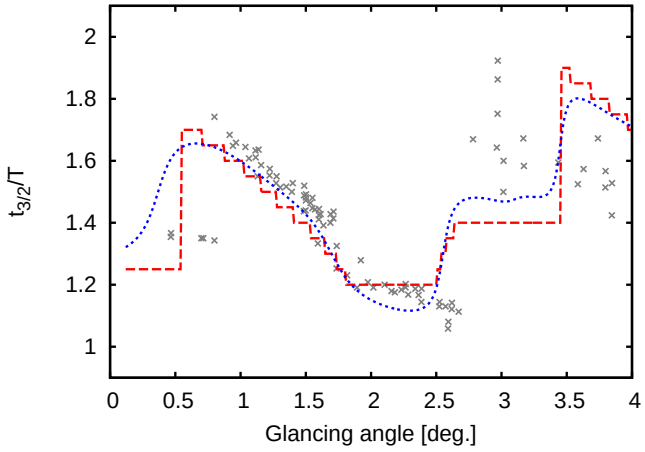

Fig. 6. Comparison of the experimental and theoretical phase of oscillations. Experimental data collected by Crook *et al.* (1989) are shown with crosess. Theoretical results obtained by the direct examination of oscillations runs are shown with the solid line, theoretical results obtained using harmonic analysis are shown with the dotted line. Thermal vibrations of atoms were ignored in the theoretical model.

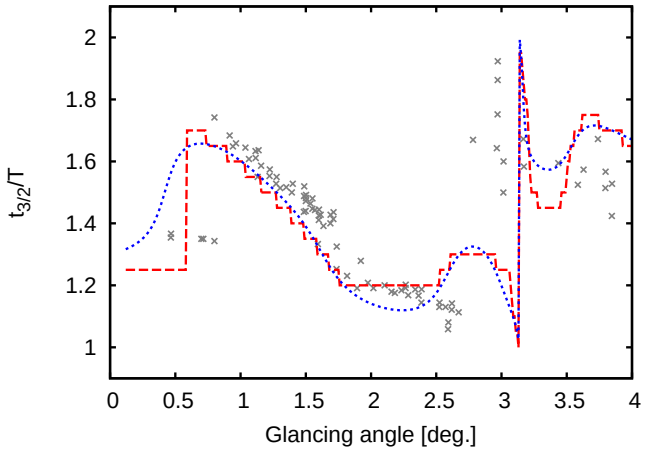

Fig. 7. The same as for Fig.6, however, theoretical results are for the model taking into account thermal vibrations of atoms. The following vaules of Debye-Waller factors were assumed: $B_{Ga} = 2.0$ Å^2 and $B_{As} = 2.7$ Å^2.

Synopsis

The phase of RHEED intensity oscillations is determined by examining the oscillation runs or by using harmonic analysis.